

Autonomous Tracking and State Estimation with Generalised Group Lasso

Rui Gao, Simo Särkkä, Rubén Claveria-Vega, and Simon Godsill

Abstract—We address the problem of autonomous tracking and state estimation for marine vessels, autonomous vehicles, and other dynamic signals under a (structured) sparsity assumption. With the aim of improving the tracking and estimation performance with respect to classical Bayesian filters and smoothers, we formulate such problems as a generalised L_2 -penalised minimisation problem, namely a dynamic generalised group Lasso problem. We first derive batch tracking and estimation methods based on a multi-block alternating direction method of multipliers algorithmic framework. For the case when the number of time points is large (e.g., thousands), we present three effective methods which solve the primal minimisation problem by augmented recursive smoothers. These smoothers are mathematically equivalent to the corresponding batch methods, but allow for low complexity implementations. The proposed methods can deal with large-scale problems without pre-processing for dimensionality reduction, which makes them attractive to address large-scale tracking and estimation problems with sparsity-inducing priors. Additionally, we establish convergence results for the proposed methods. By simulated and real-data experiments including multi-sensor range measurement problems, marine vessel tracking, autonomous vehicle tracking, and audio signal restoration, we show the effectiveness of the proposed methods.

Index Terms—Autonomous tracking, state estimation, Kalman smoother, alternating direction method of multipliers (ADMM), sparsity, group Lasso.

I. INTRODUCTION

AUTONOMOUS tracking and state estimation are active research topics with many real-world applications, including intelligent maritime navigation, autonomous vehicle tracking, and audio signal estimation [1]–[5]. The aim is to autonomously estimate and track the state (e.g., position, velocity, or direction) of the dynamic system using imperfect measurements [6]. A frequently used approach for an autonomous tracking and estimation problem is based on Bayesian filtering and smoothing. When the target dynamics and observation models are linear and Gaussian, Kalman smoother (KS) [1], [7] provides the optimal minimum mean square error estimator. In the case of non-linear dynamic systems, the iterated extended Kalman smoother (IEKS) [8], [9] makes use of local affine approximations by means of Taylor series for the non-linear functions, and then iteratively carries out KS. Sigma-point based smoothing methods [10], [11] employ sigma-points to approximate the probability density of the states, which can preserve higher order accuracy

than IEKS. Random sampling-based filters such as particle filters [12], can be used to deal with non-linear tracking situations involving potentially arbitrary nonlinearities, noise, and constraints. An optimisation-based KS method was used in [13] for tracking in collaborative sensor networks. Although these trackers and estimators are capable of utilising the measurement information to obtain the estimates, they ignore sparsity dictated by physical attributes of dynamic systems.

The motivation for our work comes from the following applications. One significant application is *marine vessel tracking* [5], [6]. Vessels are frequently pitching and rolling on the surface of the ocean, which can be modelled as sparsity in the process noise. Our methodology is also applicable to *autonomous vehicle tracking*, which enables a vehicle to autonomously avoid obstacles and maintain safe distances from other vehicles. In presence of many sudden stops (i.e., velocities are zero), the tracking accuracy can be improved by employing sparsity [14]. Other examples of tracked targets include robots [9] and unmanned aerial vehicles [15]. Another practical application is *audio signal restoration*, where typically only a few time-frequency elements are expected to be present, and thus, sparsity is an advisable assumption [16], [17]. For example, Gabor synthesis representation with sparsity constraints has been proved to be suitable for audio restoration. Similar challenges can also be found in electrocardiogram (ECG) signal analysis [18] and automatic music transcription [19]. Hence, computationally effective sparsity modelling methods are in demand.

Because sparsity may improve the tracking and estimation performance, there is a growing literature that proposes sparse regularisers such as Lasso (i.e., least absolute shrinkage and selection operator, or L_1 -regularisation) [20], [21] or total variation (TV) [22] for these applications. The Lasso methodology can be used to address L_1 -penalised target tracking or state estimation problems [23], [24]. These methods explore the trackers and estimators by merging the filtering/smoothing with L_1 -regularisation. Some research works such as [25], [26] have formulated the whole tracking and state estimation problem as an L_1 -penalised minimisation problem. Some research works [27], [28] have used sparse representation models to address visual tracking problems. While these L_1 -penalised estimators offer several benefits, they penalise individual elements of the state vector or process noise instead of groups of elements in them. Therefore, in this paper, we present new efficient methods for regularised autonomous tracking and estimation, which allow for group Lasso type of sparseness assumptions on groups of state and process noise elements.

Distinct from the existing methods [11]–[14], [18], [19],

R. Gao and S. Särkkä are with the Department of Electrical Engineering and Automation, Aalto University, Espoo, 02150 Finland (e-mail: rui.gao@aalto.fi; simo.sarkka@aalto.fi). R. Claveria-Vega and S. Godsill are with the Department of Engineering, University of Cambridge, CB2 1PZ, UK (e-mail: rmc83@cam.ac.uk; sjg@eng.cam.ac.uk).

[23]–[30], we recognise autonomous tracking and state estimation problems as a generalised L_2 -minimisation problem, which contains a wide family of sparsity structures, even including various L_1 -regularisation approaches. The resulting problem is difficult to solve due to its non-smoothness and/or even non-convexity. Splitting-based optimisation methods [31] such as multi-block alternating direction method of multipliers (ADMM) [32], are methods with such decomposition properties. However, when the number of time points is large, the naive use of the batch optimization methods suffers from the curse of dimensionality, since these methods do not explicitly leverage the structure induced by the implied dynamic model [14]. This often causes the existing methods to be intractable due to massive computational costs. Hence, we develop computationally efficient methods to improve the tracking and estimation performance.

This paper focuses on autonomous tracking and state estimation problems with sparsity-inducing priors. Since splitting-based methods can deal with sparsity-promoting regularisers and Bayesian filtering/smoothing is suitable for problems with an inherent temporal structure, we present the efficient smoothing-and-splitting tracking and estimation methods to solve such problems, also called as *dynamic generalised group Lasso* methods, and then prove their convergence under mild conditions. Our experiments demonstrate the promising performance of the methods in both simulated data and real-world applications. In summary, the main contributions are:

- i) We formulate a class of regularised autonomous tracking and state estimation problems as a generalised L_2 -minimisation problem. Special cases of the framework are Lasso, isotropic TV, anisotropic TV, fused Lasso, group Lasso, and sparse group Lasso.
- ii) For both linear and non-linear dynamic systems, we present batch multi-block ADMM (mADMM) methods to solve the resulting problems.
- iii) We develop the new KS-mADMM, Gauss–Newton IEKS-mADMM (GN-IEKS-mADMM), and Levenberg–Marquardt IEKS-mADMM (LM-IEKS-mADMM), which use the recursive smoothers on new augmented state-space models to compute the primal variable.
- iv) We prove the convergence of the proposed methods.
- v) We experiment the proposed methods in real-world applications of marine vessel tracking, autonomous vehicle tracking, and audio signal restoration.

The rest of this paper is structured as follows. In Section II, we formulate the sparse autonomous tracking and state estimation problem as a generalised L_2 -minimisation problem. Particularly, we present a broad class of regulariser configurations parametrised by two sets of matrices and a set of vectors. We introduce the batch tracking and estimation methods in Section III. Corresponding to the batch methods, we present three augmented recursive smoothing methods in Section IV. In Section V, we establish the convergence. In Section VI, we report numerical results on simulated data and real-life applications. Section VII draws concluding remarks.

The notation is as follows. Matrices \mathbf{X} and vectors \mathbf{x} are indicated in boldface. $(\cdot)^\top$ stands for transposition, and

$(\cdot)^{-1}$ represents matrix inversion. The \mathbf{R} -weighted norm of a vector \mathbf{x} is denoted by $\|\mathbf{x}\|_{\mathbf{R}} = \sqrt{\mathbf{x}^\top \mathbf{R} \mathbf{x}}$. $\|\mathbf{x}\|_1 = \sum |x_i|$ denotes L_1 -norm, and $\|\mathbf{x}\|_2 = \sqrt{\sum_i x_i^2}$ denotes L_2 -norm. $\mathbf{X}_{g,t}$ is the (g,t) :th element of matrix \mathbf{X} , and $\mathbf{x}^{(k)}$ denotes the value of \mathbf{x} at k :th iteration. $\text{vec}(\cdot)$ represents a vectorisation operator, $\text{diag}(\cdot)$ represents a block diagonal matrix operator with the elements in its argument on the diagonal, $\mathbf{x}_{1:T} = \text{vec}(\mathbf{x}_1, \dots, \mathbf{x}_T)$. $\partial\phi(\mathbf{x})$ denotes a sub-gradient of ϕ . \mathbf{J}_ϕ is the Jacobian of $\phi(\mathbf{x})$. $p(\mathbf{x})$ represents probability density function (pdf) of \mathbf{x} and $\mathcal{N}(\mathbf{x} | \mathbf{m}, \mathbf{P})$ denotes a Gaussian pdf with mean \mathbf{m} and covariance \mathbf{P} evaluated at \mathbf{x} .

II. PROBLEM STATEMENT

Let $\mathbf{y}_t \in \mathbb{R}^{N_y}$ be a measurement of a dynamic system and $\mathbf{x}_t \in \mathbb{R}^{N_x}$ be an unknown state (sometimes called the source or signal). The state and measurement are related according to a dynamic state-space model of the form

$$\begin{aligned}\mathbf{x}_t &= \mathbf{a}_t(\mathbf{x}_{t-1}) + \mathbf{q}_t, \\ \mathbf{y}_t &= \mathbf{h}_t(\mathbf{x}_t) + \mathbf{r}_t,\end{aligned}\tag{1}$$

where $\mathbf{h}_t : \mathbb{R}^{N_x} \rightarrow \mathbb{R}^{N_y}$ and $\mathbf{a}_t : \mathbb{R}^{N_x} \rightarrow \mathbb{R}^{N_x}$ are the measurement and state transition functions, respectively, and $t = 1, \dots, T$ is the time step number. The process and measurement noises $\mathbf{q}_t \sim \mathcal{N}(\mathbf{0}, \mathbf{Q}_t)$ and $\mathbf{r}_t \sim \mathcal{N}(\mathbf{0}, \mathbf{R}_t)$ are assumed to be zero-mean Gaussian with covariances \mathbf{Q}_t and \mathbf{R}_t , respectively. The initial condition at $t = 1$ is given by $\mathbf{x}_1 \sim \mathcal{N}(\mathbf{m}_1, \mathbf{P}_1)$. The goal here is to obtain the “best estimate” of $\mathbf{x}_{1:T}$ from imperfect measurements.

For computing $\mathbf{x}_{1:T}$ with sparsity-inducing priors, we define a set of matrices $\{\mathbf{G}_{g,t} \in \mathbb{R}^{P_g \times N_x} \mid g = 1, \dots, N_g\}$, matrices \mathbf{B}_t , vectors \mathbf{d}_t , for $t = 1, \dots, T$, and impose sparsity on the groups of elements of the state or the process noise. Mathematically, the problem of computing the state estimate $\mathbf{x}_{1:T}^*$ is formulated as

$$\begin{aligned}\mathbf{x}_{1:T}^* &= \arg \min_{\mathbf{x}_{1:T}} \frac{1}{2} \sum_{t=1}^T \|\mathbf{y}_t - \mathbf{h}_t(\mathbf{x}_t)\|_{\mathbf{R}_t^{-1}}^2 \\ &+ \frac{1}{2} \sum_{t=2}^T \|\mathbf{x}_t - \mathbf{a}_t(\mathbf{x}_{t-1})\|_{\mathbf{Q}_t^{-1}}^2 + \frac{1}{2} \|\mathbf{x}_1 - \mathbf{m}_1\|_{\mathbf{P}_1^{-1}}^2 \\ &+ \sum_{t=1}^T \sum_{g=1}^{N_g} \mu \|\mathbf{G}_{g,t}(\mathbf{x}_t - \mathbf{B}_t \mathbf{x}_{t-1} - \mathbf{d}_t)\|_2,\end{aligned}\tag{2}$$

where $\mu > 0$ is a penalty parameter.

A merit of our formulation is its flexibility, because the selections of $\mathbf{G}_{g,t}$, \mathbf{B}_t , and \mathbf{d}_t can be adjusted to represent different regularisers. With matrix $\mathbf{G}_{g,t}$, the formulation (2) accommodates a large class of sparsity-promoting regularisers (e.g., Lasso, isotropic TV, anisotropic TV, fused Lasso, group Lasso, and sparse group Lasso). A list of such regularisers is reported in Table I. Meanwhile, the formulation (2) also allows for putting sparsity assumptions on the state or the process noise by different selections of \mathbf{B}_t and \mathbf{d}_t .

- i) $\mathbf{B}_t = \mathbf{0}$ and $\mathbf{d}_t = \mathbf{0}$, which corresponds to sparsity assumption on \mathbf{x}_t ;

TABLE I
EXAMPLES OF SPARSITY-PROMOTING REGULARISERS THAT ARE
INCLUDED IN THE PRESENT FRAMEWORK.

Regularisation	$\mathbf{G}_{g,t}$ descriptions
L_2 -regularisation	$\mathbf{G}_{g,t}$ is an identity matrix
Lasso	$N_g = N_x$, $P_g = 1$ for all g , $\mathbf{G}_{g,t}$ has 1 at g :th column and zeros otherwise.
Isotopic TV	$N_g = 1$, $P_1 = N_x - 1$ $\mathbf{G}_{1,t}$ encodes a finite difference operator.
Anisotropic TV	$\mathbf{G}_{g,t}$ encodes the g :th row of a finite difference operator.
Fused Lasso	$g = 1, \dots, N_x$, $P_g = 1$ for all g , $\mathbf{G}_{g,t}$ has 1 at g :th column and zeros otherwise; $g = N_x + 1, \dots, N_g$, $\mathbf{G}_{g,t}$ encodes the g :th row of a finite difference operator.
Group Lasso	$\mathbf{G}_{g,t}$ has 1, corresponding to the selected elements of \mathbf{x}_t in the group and zeros otherwise.
Sparse group Lasso	$g = 1, \dots, N_x$, $P_g = 1$, $\mathbf{G}_{g,t}$ has 1 at g :th column and zeros otherwise; $g = N_x + 1, \dots, N_g$, $\mathbf{G}_{g,t}$ has the same setting with Group Lasso.

- ii) $(\mathbf{B}_t \mathbf{x}_{t-1} + \mathbf{d}_t)$ as the affine approximation of $\mathbf{a}_t(\mathbf{x}_{t-1})$, which corresponds to the sparsity assumption on \mathbf{q}_t (see Section IV-B).

A simple, yet illustrative, example can be found in autonomous vehicle tracking. When there are stop-and-go points (e.g. vehicle stops) in the data then the zero-velocity and zero-angle values at those time points can be grouped together via the L_2 -norm and $\mathbf{G}_{g,t}$, that is, three elements can be forced to be equal to zero at the same time. Another extension application is an audio restoration, where the matrices $\mathbf{G}_{g,t}$ are defined so that only two elements of the state \mathbf{x}_t – corresponding to the real and imaginary parts of a synthesis coefficient – are extracted at a time step. Thus, these pairs, which are associated to the same time-frequency basis functions, tend to be selected or discarded together.

The objective (2) is more difficult to solve than the common L_2 -minimisation problem (which corresponds to $\mathbf{G}_{g,t} = \mathbf{I}$, where \mathbf{I} is an identity matrix) or the squared L_2 -minimisation problem (the problem with $\|\mathbf{G}_{g,t}(\cdot)\|_2^2$), since the penalty term $\|\mathbf{G}_{g,t}(\cdot)\|_2$ is non-smooth and $\mathbf{G}_{g,t}$ is possibly rank-deficient matrix. In this paper, we first derive batch tracking and estimation methods, which are based on the batch computation of the state sequence. In an effort to speed up the batch methods, we then propose augmented recursive smoothing based methods for the primal variable update.

III. BATCH TRACKING AND ESTIMATION METHODS

In this section, we introduce the multi-block ADMM framework. Based on this framework, we derive batch algorithms for solving the regularised tracking and state estimation problem.

A. The General Multi-block ADMM (mADMM) Framework

The methods that we develop are based on the multi-block ADMM [32]. The multi-block ADMM provides an algorithmic framework which is applicable to problems of the form (2), and it can be instantiated by defining the auxiliary variables and their update steps. We introduce auxiliary variables \mathbf{v}_t and

$\mathbf{w}_{g,t}$, $g = 1, \dots, N_g$, from $t = 1$ to $t = T$, and then build the following constraints

$$\begin{aligned} \mathbf{x}_t - \mathbf{B}_t \mathbf{x}_{t-1} - \mathbf{d}_t &= \mathbf{v}_t, \\ \mathbf{w}_{1,t} &= \mathbf{G}_{1,t} \mathbf{v}_t, \\ &\vdots \\ \mathbf{w}_{N_g,t} &= \mathbf{G}_{N_g,t} \mathbf{v}_t. \end{aligned} \quad (3)$$

Note that in (3) we could alternatively introduce auxiliary variables $\tilde{\mathbf{w}}_{g,t} = \mathbf{G}_{g,t}(\mathbf{x}_t - \mathbf{B}_t \mathbf{x}_{t-1} - \mathbf{d}_t)$, but this replacement would require $\mathbf{G}_{g,t}$ to be invertible when using the augmented recursive smoothers later on. To avoid such restrictions, we employ variables \mathbf{v}_t and $\mathbf{w}_{g,t}$ to build the more general constraints in this paper.

For simplicity of notation, we denote $\underline{\mathbf{w}}_t = [\mathbf{w}_{1,t}, \dots, \mathbf{w}_{N_g,t}]$, $\underline{\mathbf{G}}_t = [\mathbf{G}_{1,t}, \dots, \mathbf{G}_{N_g,t}]$, and then solve (2), using an equivalent constrained optimisation problem

$$\begin{aligned} \min_{\substack{\mathbf{x}_{1:T}, \mathbf{v}_{1:T}, \\ \mathbf{w}_{1:T}}} & \frac{1}{2} \sum_{t=1}^T \|\mathbf{y}_t - \mathbf{h}_t(\mathbf{x}_t)\|_{\mathbf{R}_t^{-1}}^2 + \sum_{t=1}^T \sum_{g=1}^{N_g} \mu \|\mathbf{w}_{g,t}\|_2 \\ & + \frac{1}{2} \sum_{t=2}^T \|\mathbf{x}_t - \mathbf{a}_t(\mathbf{x}_{t-1})\|_{\mathbf{Q}_t^{-1}}^2 + \frac{1}{2} \|\mathbf{x}_1 - \mathbf{m}_1\|_{\mathbf{P}_1^{-1}}^2 \\ \text{s.t.} & \begin{bmatrix} \mathbf{x}_t - \mathbf{B}_t \mathbf{x}_{t-1} - \mathbf{d}_t \\ \underline{\mathbf{w}}_t \end{bmatrix} = \begin{bmatrix} \mathbf{I} \\ \underline{\mathbf{G}}_t \end{bmatrix} \mathbf{v}_t, \quad t = 1, \dots, T. \end{aligned} \quad (4)$$

The variables $\mathbf{x}_{1:T}$, $\mathbf{w}_{1:T} = \text{vec}(\mathbf{w}_1, \dots, \mathbf{w}_T)$, and $\mathbf{v}_{1:T}$ can be dealt with by defining the augmented Lagrangian function

$$\begin{aligned} \mathcal{L}_\gamma(\mathbf{x}_{1:T}, \mathbf{w}_{1:T}, \mathbf{v}_{1:T}; \boldsymbol{\eta}_{1:T}) &\triangleq \frac{1}{2} \sum_{t=1}^T \|\mathbf{y}_t - \mathbf{h}_t(\mathbf{x}_t)\|_{\mathbf{R}_t^{-1}}^2 \\ & + \frac{1}{2} \sum_{t=2}^T \|\mathbf{x}_t - \mathbf{a}_t(\mathbf{x}_{t-1})\|_{\mathbf{Q}_t^{-1}}^2 + \frac{1}{2} \|\mathbf{x}_1 - \mathbf{m}_1\|_{\mathbf{P}_1^{-1}}^2 \\ & + \sum_{t=1}^T \sum_{g=1}^{N_g} \mu \|\mathbf{w}_{g,t}\|_2 + \sum_{t=1}^T \boldsymbol{\eta}_t^\top \left(\begin{bmatrix} \mathbf{u}_t \\ \underline{\mathbf{w}}_t \end{bmatrix} - \begin{bmatrix} \mathbf{I} \\ \underline{\mathbf{G}}_t \end{bmatrix} \mathbf{v}_t \right) \\ & + \sum_{t=1}^T \frac{\gamma}{2} \left\| \begin{bmatrix} \mathbf{u}_t \\ \underline{\mathbf{w}}_t \end{bmatrix} - \begin{bmatrix} \mathbf{I} \\ \underline{\mathbf{G}}_t \end{bmatrix} \mathbf{v}_t \right\|_2^2, \end{aligned} \quad (5)$$

where $\mathbf{u}_t = \mathbf{x}_t - \mathbf{B}_t \mathbf{x}_{t-1} - \mathbf{d}_t$, $\boldsymbol{\eta}_t \in \mathbb{R}^{(N_x + P \times N_g)}$ is a Lagrangian multiplier, and $\gamma > 0$ is a penalty parameter.

The multi-block ADMM (mADMM) framework minimises the function \mathcal{L}_γ by alternating the $\mathbf{x}_{1:T}$ -minimisation step, the $\mathbf{w}_{1:T}$ -minimisation step, the $\mathbf{v}_{1:T}$ -minimisation step, and the dual variable $\boldsymbol{\eta}_{1:T}$ update step. Given $(\mathbf{x}_{1:T}^{(k)}, \mathbf{w}_{1:T}^{(k)}, \mathbf{v}_{1:T}^{(k)}, \boldsymbol{\eta}_{1:T}^{(k)})$, the iteration of mADMM has the following steps:

$$\begin{aligned} \mathbf{x}_{1:T}^{(k+1)} &= \arg \min_{\mathbf{x}_{1:T}} \sum_{t=1}^T \frac{1}{2} \|\mathbf{y}_t - \mathbf{h}_t(\mathbf{x}_t)\|_{\mathbf{R}_t^{-1}}^2 + \frac{1}{2} \|\mathbf{x}_1 - \mathbf{m}_1\|_{\mathbf{P}_1^{-1}}^2 \\ & + \frac{1}{2} \sum_{t=2}^T \|\mathbf{x}_t - \mathbf{a}_t(\mathbf{x}_{t-1})\|_{\mathbf{Q}_t^{-1}}^2 + \frac{\gamma}{2} \sum_{t=1}^T \left\| \mathbf{u}_t - \mathbf{v}_t^{(k)} + \frac{\bar{\boldsymbol{\eta}}_t^{(k)}}{\gamma} \right\|_2^2, \end{aligned} \quad (6a)$$

$$\mathbf{w}_t^{(k+1)} = \arg \min_{\mathbf{w}_t} \sum_{g=1}^{N_g} \mu \|\mathbf{w}_{g,t}\|_2 + \frac{\gamma}{2} \left\| \underline{\mathbf{w}}_t - \underline{\mathbf{G}}_t \mathbf{v}_t^{(k)} + \frac{\underline{\boldsymbol{\eta}}_t^{(k)}}{\gamma} \right\|_2^2 \quad (6b)$$

$$\mathbf{v}_t^{(k+1)} = \arg \min_{\mathbf{v}_t} \frac{\gamma}{2} \left\| \begin{bmatrix} \mathbf{u}_t \\ \underline{\mathbf{w}}_t \end{bmatrix} - \begin{bmatrix} \mathbf{I} \\ \underline{\mathbf{G}}_t \end{bmatrix} \mathbf{v}_t + \underline{\boldsymbol{\eta}}_t / \gamma \right\|_2^2, \quad (6c)$$

$$\underline{\boldsymbol{\eta}}_t^{(k+1)} = \underline{\boldsymbol{\eta}}_t^{(k)} + \gamma \left(\begin{bmatrix} \mathbf{u}_t^{(k+1)} \\ \underline{\mathbf{w}}_t^{(k+1)} \end{bmatrix} - \begin{bmatrix} \mathbf{I} \\ \underline{\mathbf{G}}_t^{(k+1)} \end{bmatrix} \mathbf{v}_t^{(k+1)} \right), \quad (6d)$$

where $\underline{\boldsymbol{\eta}}_t = \text{vec}(\underline{\boldsymbol{\eta}}_t, \underline{\boldsymbol{\eta}}_{1,t}, \dots, \underline{\boldsymbol{\eta}}_{N_g,t})$. We solve the \mathbf{w}_t , \mathbf{v}_t , and $\underline{\boldsymbol{\eta}}_t$ subproblems for each $t = 1, \dots, T$, respectively. The \mathbf{w}_t -subproblem and \mathbf{v}_t -subproblem have the solutions

$$\mathbf{w}_t^{(k+1)} = \mathcal{S}_{\mu/\gamma} \left(\underline{\mathbf{G}}_{g,t} \mathbf{v}_t^{(k)} - \underline{\boldsymbol{\eta}}_{g,t}^{(k)} / \gamma \right), \quad (7a)$$

$$\mathbf{v}_t^{(k+1)} = \frac{1}{\gamma} (\mathbf{I} + \underline{\mathbf{G}}_t^\top \underline{\mathbf{G}}_t)^{-1} \left(\begin{bmatrix} \mathbf{I} \\ \underline{\mathbf{G}}_t \end{bmatrix}^\top \left(\gamma \begin{bmatrix} \mathbf{u}_t^{(k+1)} \\ \underline{\mathbf{w}}_t^{(k+1)} \end{bmatrix} + \underline{\boldsymbol{\eta}}_t^{(k)} \right) \right), \quad (7b)$$

where $\mathcal{S}_{\mu/\gamma}(\cdot)$ is the shrinkage operator [33]. In the following, we present batch methods to solve the $\mathbf{x}_{1:T}$ -subproblem.

B. Batch Solution for Affine Systems

The first batch method we explore is for affine Gaussian systems, which have the form

$$\mathbf{a}_t(\mathbf{x}_{t-1}) = \mathbf{A}_t \mathbf{x}_{t-1} + \mathbf{b}_t, \quad \mathbf{h}_t(\mathbf{x}_t) = \mathbf{H}_t \mathbf{x}_t + \mathbf{e}_t, \quad (8)$$

where $\mathbf{A}_t \in \mathbb{R}^{N_x \times N_x}$, $\mathbf{H}_t \in \mathbb{R}^{N_y \times N_x}$ are the transition and measurement matrices, and \mathbf{b}_t , \mathbf{e}_t are bias terms. Now, we stack all the state variables into the single variables, and rewrite the $\mathbf{x}_{1:T}$ -subproblem (6a) in the form

$$\mathbf{x}^* = \arg \min_{\mathbf{x}} \frac{1}{2} \|\mathbf{y} - \mathbf{H} \mathbf{x} - \mathbf{e}\|_{\mathbf{R}^{-1}}^2 + \frac{1}{2} \|\mathbf{m} - \mathbf{A} \mathbf{x} - \mathbf{b}\|_{\mathbf{Q}^{-1}}^2 + \frac{\gamma}{2} \left\| \Phi \mathbf{x} - \mathbf{d} - \mathbf{v}^{(k)} + \bar{\boldsymbol{\eta}}^{(k)} / \gamma \right\|_2^2, \quad (9)$$

where we have denoted $\mathbf{x} \triangleq \mathbf{x}_{1:T}$ and the rest of the terms \mathbf{y} , \mathbf{e} , \mathbf{m} , \mathbf{d} , \mathbf{v} , $\bar{\boldsymbol{\eta}}$, \mathbf{H} , \mathbf{R} , \mathbf{Q} , \mathbf{A} , Φ are defined analogously to [14]. By setting the derivative to zero, the solution is

$$\begin{aligned} \mathbf{x}^{(k+1)} &= (\mathbf{H}^\top \mathbf{R}^{-1} \mathbf{H} + \mathbf{A}^\top \mathbf{Q}^{-1} \mathbf{A} + \gamma \Phi^\top \Phi)^{-1} \\ &\times (\mathbf{H}^\top \mathbf{R}^{-1} (\mathbf{y} - \mathbf{e}) + \mathbf{A}^\top \mathbf{Q}^{-1} (\mathbf{m} - \mathbf{b}) \\ &+ \gamma \Phi^\top (\mathbf{d} + \mathbf{v}^{(k)} - \bar{\boldsymbol{\eta}}^{(k)} / \gamma)). \end{aligned} \quad (10)$$

In other words, computing the \mathbf{x} -minimisation amounts to solving a linear system with positive definite coefficient matrix $\mathbf{H}^\top \mathbf{R}^{-1} \mathbf{H} + \mathbf{A}^\top \mathbf{Q}^{-1} \mathbf{A} + \gamma \Phi^\top \Phi$. When the matrix inverse exists, the \mathbf{x} -subproblem has a unique solution. Additionally, with a sparsity assumption on the states \mathbf{x}_t , Φ is an identity matrix, and \mathbf{d} is a zero vector. When the noise \mathbf{q}_t is sparse, we can set

$$\Phi = \Psi, \quad \mathbf{d} = \mathbf{m} - \mathbf{b}, \quad (11)$$

which corresponds to the setting of \mathbf{B}_t and \mathbf{d}_t discussed in Section II.

The disadvantage of the batch solution is that it requires an extensive amount of computations. With increasing time steps, the computation by stacking the states of all T time

steps is computationally demanding. As we will see in Section IV-A, the use of an augmented recursive smoother, which is mathematically equivalent to the batch method, will improve the computational performance significantly.

C. Gauss–Newton (GN) for Non-linear Systems

When the system in (1) is non-linear, we use a similar batch notation as in the affine case, and additionally define the non-linear functions

$$\begin{aligned} \mathbf{a}(\mathbf{x}) &= \text{vec}(\mathbf{x}_1, \mathbf{x}_2 - \mathbf{a}_2(\mathbf{x}_1), \dots, \mathbf{x}_T - \mathbf{a}_T(\mathbf{x}_{T-1})), \\ \mathbf{h}(\mathbf{x}) &= \text{vec}(\mathbf{h}_1(\mathbf{x}_1), \dots, \mathbf{h}_T(\mathbf{x}_T)). \end{aligned} \quad (12)$$

The primal $\mathbf{x}_{1:T}$ -subproblem then has the form

$$\mathbf{x}^{(k+1)} = \arg \min_{\mathbf{x}} \theta(\mathbf{x}), \quad (13)$$

$$\begin{aligned} \theta(\mathbf{x}) &= \frac{1}{2} \|\mathbf{y} - \mathbf{h}(\mathbf{x})\|_{\mathbf{R}^{-1}}^2 + \frac{1}{2} \|\mathbf{m} - \mathbf{a}(\mathbf{x})\|_{\mathbf{Q}^{-1}}^2 \\ &+ \frac{\gamma}{2} \left\| \Phi \mathbf{x} - \mathbf{d} - \mathbf{v}^{(k)} + \bar{\boldsymbol{\eta}}^{(k)} / \gamma \right\|_2^2. \end{aligned} \quad (14)$$

The function $\theta(\mathbf{x})$ can now be minimised by the Gauss–Newton (GN) method [31]. In GN, we first linearise the non-linear functions $\mathbf{a}(\mathbf{x})$ and $\mathbf{h}(\mathbf{x})$, and then replace them in $\theta(\mathbf{x})$ by the linear (or actually affine) approximations. The GN iteration then becomes

$$\begin{aligned} \mathbf{x}^{(k,i+1)} &= \left(\mathbf{J}_\theta^\top \mathbf{J}_\theta(\mathbf{x}^{(k,i)}) \right)^{-1} \left[\mathbf{J}_h^\top(\mathbf{x}^{(k,i)}) \mathbf{R}^{-1} (\mathbf{y} - \mathbf{h}(\mathbf{x}^{(k,i)})) \right. \\ &+ \mathbf{J}_h(\mathbf{x}^{(k,i)}) \mathbf{x}^{(k,i)} \left. + \mathbf{J}_a^\top(\mathbf{x}^{(k,i)}) \mathbf{Q}^{-1} (\mathbf{m} - \mathbf{a}(\mathbf{x}^{(k,i)})) \right. \\ &+ \left. \mathbf{J}_a(\mathbf{x}^{(k,i)}) \mathbf{x}^{(k,i)} \right] + \gamma \Phi^\top (\mathbf{d} + \mathbf{v}^{(k)} - \bar{\boldsymbol{\eta}}^{(k)} / \gamma). \end{aligned} \quad (15)$$

where

$$\mathbf{J}_\theta^\top \mathbf{J}_\theta(\mathbf{x}) = \mathbf{J}_h^\top(\mathbf{x}) \mathbf{R}^{-1} \mathbf{J}_h(\mathbf{x}) + \mathbf{J}_a^\top(\mathbf{x}) \mathbf{Q}^{-1} \mathbf{J}_a(\mathbf{x}) + \gamma \Phi^\top \Phi.$$

The above computations are carried out iteratively until a maximum number of iterations I_{\max} is reached. We take the solution $\mathbf{x}^{(k, I_{\max})}$ as the next iterate $\mathbf{x}^{(k+1)}$. While GN avoids the trouble of computing the Hessians of the model functions, it has problems when the Jacobians are rank-deficient. The Levenberg–Marquardt method is introduced next to address this problem.

D. Levenberg–Marquardt (LM) Method

The Levenberg–Marquardt (LM) method [34], also called as the regularised or damped GN method, improves the performance of GN by using an additional regularisation term. With damping factors $\lambda^{(i)} > 0$ and a sequence of positive definite regularisation matrices $\mathbf{S}^{(i)}$, the function $\theta(\mathbf{x})$ can be approximated by

$$\begin{aligned} \theta(\mathbf{x}) &\approx \frac{1}{2} \left\| \mathbf{y} - \mathbf{h}(\mathbf{x}^{(i)}) + \mathbf{J}_h(\mathbf{x}^{(i)}) (\mathbf{x} - \mathbf{x}^{(i)}) \right\|_{\mathbf{R}^{-1}}^2 \\ &+ \frac{1}{2} \left\| \mathbf{m} - \mathbf{a}(\mathbf{x}^{(i)}) + \mathbf{J}_a(\mathbf{x}^{(i)}) (\mathbf{x} - \mathbf{x}^{(i)}) \right\|_{\mathbf{Q}^{-1}}^2 \\ &+ \frac{\gamma}{2} \left\| \Phi \mathbf{x} - \mathbf{d} - \mathbf{v}^{(k)} + \bar{\boldsymbol{\eta}}^{(k)} / \gamma \right\|_2^2 + \frac{\lambda^{(i)}}{2} \left\| \mathbf{x} - \mathbf{x}^{(i)} \right\|_{[\mathbf{S}^{(i)}]^{-1}}^2. \end{aligned} \quad (16)$$

Using the minimum of this approximate cost function at each step i as the next iterate, we get the following iteration:

$$\begin{aligned} \mathbf{x}^{(k,i+1)} = & \left(\mathbf{J}_\theta^\top \mathbf{J}_\theta (\mathbf{x}^{(k,i)}) + \lambda^{(i)} [\mathbf{S}^{(i)}]^{-1} \right)^{-1} \\ & \left[\mathbf{J}_h^\top (\mathbf{x}^{(k,i)}) \mathbf{R}^{-1} \left(\mathbf{y} - \mathbf{h}(\mathbf{x}^{(k,i)}) + \mathbf{J}_h (\mathbf{x}^{(k,i)}) \mathbf{x}^{(k,i)} \right) \right. \\ & + \mathbf{J}_a^\top (\mathbf{x}^{(k,i)}) \mathbf{Q}^{-1} \left(\mathbf{m} - \mathbf{a}(\mathbf{x}^{(k,i)}) + \mathbf{J}_a (\mathbf{x}^{(k,i)}) \mathbf{x}^{(k,i)} \right) \\ & \left. + \gamma \Phi^\top \left(\mathbf{d} + \mathbf{v}^{(k)} - \bar{\boldsymbol{\eta}}^{(k)} / \gamma \right) \right], \end{aligned} \quad (17)$$

which is the LM method, when augmented with an adaptation scheme for the regularisation parameters $\lambda^{(i)} > 0$. The regularisation parameter here helps to overcome some problematic cases, for example, the case when $\mathbf{J}_\theta^\top \mathbf{J}_\theta (\mathbf{x})$ is rank-deficient, by ensuring the existence of the unique minimum of the approximate cost function.

At each mADMM iteration, the computation in the $\mathbf{x}_{1:T}$ -subproblem, such as (10), (15), and (17), has a high cost when T is large (e.g., $T = 10^8$). It typically takes at least $\mathcal{O}(N_x^3 T^3)$ operations. As the main computational demand is indeed in updating $\mathbf{x}_{1:T}$, in the next section, we develop an efficient augmented recursive smoother solution for it.

IV. AUGMENTED RECURSIVE SMOOTHERS

In the section, we will present augmented KS, GN-IEKS, and LM-IEKS methods for solving the $\mathbf{x}_{1:T}$ -subproblem.

A. Kalman Smoother (KS) for Affine Systems

In the affine model case, the computation for the $\mathbf{x}_{1:T}$ -subproblem involves minimisation of a quadratic optimisation problem, which can also be efficiently solved by Bayesian filtering/smoothing type of recursive methods. To connect the above batch method to KS, we rewrite the batch minimisation problem (9) as

$$\begin{aligned} \mathbf{x}_{1:T}^* = & \arg \min_{\mathbf{x}_{1:T}} \frac{1}{2} \sum_{t=1}^T \|\mathbf{y}_t - \mathbf{H}_t \mathbf{x}_t - \mathbf{e}_t\|_{\mathbf{R}_t^{-1}}^2 \\ & + \frac{1}{2} \sum_{t=2}^T \|\mathbf{x}_t - \mathbf{A}_t \mathbf{x}_{t-1} - \mathbf{b}_t\|_{\mathbf{Q}_t^{-1}}^2 + \frac{1}{2} \|\mathbf{x}_1 - \mathbf{m}_1\|_{\mathbf{P}_1^{-1}}^2 \\ & + \frac{\gamma}{2} \sum_{t=2}^T \|\mathbf{x}_t - \mathbf{B}_t \mathbf{x}_{t-1} - \mathbf{d}_t - \mathbf{v}_t + \bar{\boldsymbol{\eta}}_t / \gamma\|_2^2 \\ & + \frac{\gamma}{2} \|\mathbf{x}_1 - \mathbf{m}_1 - \mathbf{v}_1 + \bar{\boldsymbol{\eta}}_1 / \gamma\|_2^2. \end{aligned} \quad (18)$$

When $\mathbf{B}_t = \mathbf{0}$ and $\mathbf{d}_t = \mathbf{0}$, the cost function corresponds to the cost function minimised by a Kalman smoother (KS), which leads to a similar method as was presented in [14]. When \mathbf{B}_t and \mathbf{d}_t are non-zero, the situation is more complicated as we cannot have two dynamic models in a state-space model. However, in that case we can combine the terms in the pairs $\frac{1}{2} \|\mathbf{x}_t - \mathbf{A}_t \mathbf{x}_{t-1} - \mathbf{b}_t\|_{\mathbf{Q}_t^{-1}}^2$ and $\frac{1}{2} \|\mathbf{x}_t - \mathbf{B}_t \mathbf{x}_{t-1} - \mathbf{d}_t - \mathbf{v}_t + \bar{\boldsymbol{\eta}}_t / \gamma\|_2^2$, along with $\frac{1}{2} \|\mathbf{x}_1 - \mathbf{m}_1\|_{\mathbf{P}_1^{-1}}^2$ and $\frac{1}{2} \|\mathbf{x}_1 - \mathbf{m}_1 - \mathbf{v}_1 + \bar{\boldsymbol{\eta}}_1 / \gamma\|_2^2$ into single terms.

To build the new dynamic state-space model, we combine matrices \mathbf{A}_t and \mathbf{B}_t to an artificial transition matrix $\tilde{\mathbf{A}}_t$, fuse \mathbf{b}_t and $(\mathbf{d}_t + \mathbf{v}_t - \bar{\boldsymbol{\eta}}_t / \gamma)$ to an artificial bias $\tilde{\mathbf{b}}_t$, and then introduce the covariance $\tilde{\mathbf{Q}}_t$, which yields

$$\begin{aligned} \tilde{\mathbf{A}}_t &= (\mathbf{Q}_t^{-1} + \gamma \mathbf{I})^{-1} (\mathbf{Q}_t^{-1} \mathbf{A}_t + \gamma \mathbf{B}_t), \\ \tilde{\mathbf{b}}_t &= (\mathbf{Q}_t^{-1} + \gamma \mathbf{I})^{-1} (\mathbf{Q}_t^{-1} \mathbf{b}_t + \gamma \mathbf{d}_t + \gamma \mathbf{v}_t - \bar{\boldsymbol{\eta}}_t), \\ \tilde{\mathbf{Q}}_t^{-1} &= \mathbf{Q}_t^{-1} + \gamma \mathbf{I}. \end{aligned} \quad (19)$$

The new artificial dynamic model (19) allows us to use KS to solve the minimisation problem. The problem (18) becomes

$$\begin{aligned} \mathbf{x}_{1:T}^* = & \arg \min_{\mathbf{x}_{1:T}} \frac{1}{2} \sum_{t=1}^T \|\mathbf{y}_t - \mathbf{H}_t \mathbf{x}_t - \mathbf{e}_t\|_{\mathbf{R}_t^{-1}}^2 \\ & + \frac{1}{2} \|\mathbf{x}_t - \tilde{\mathbf{A}}_t \mathbf{x}_{t-1} - \tilde{\mathbf{b}}_t\|_{\tilde{\mathbf{Q}}_t^{-1}}^2 + \frac{1}{2} \|\mathbf{x}_1 - \tilde{\mathbf{m}}_1\|_{\tilde{\mathbf{P}}_1^{-1}}^2, \end{aligned} \quad (20)$$

which corresponds to a state-space model, where additionally the initial state has mean $\tilde{\mathbf{m}}_1 = (\mathbf{P}_1^{-1} + \gamma \mathbf{I})^{-1} (\mathbf{P}_1^{-1} \mathbf{m}_1 + \gamma \mathbf{m}_1 + \gamma \mathbf{v}_1 - \bar{\boldsymbol{\eta}}_1)$ and covariance $\tilde{\mathbf{P}}_1^{-1} = \mathbf{P}_1^{-1} + \gamma \mathbf{I}$. The solution in (20) can be then computed by running KS on the augmented state-space model

$$p(\mathbf{x}_t | \mathbf{x}_{t-1}) = \mathcal{N}(\mathbf{x}_t | \tilde{\mathbf{A}}_t \mathbf{x}_{t-1} + \tilde{\mathbf{b}}_t, \tilde{\mathbf{Q}}_t), \quad (21a)$$

$$p(\mathbf{y}_t | \mathbf{x}_t) = \mathcal{N}(\mathbf{y}_t | \mathbf{H}_t \mathbf{x}_t + \mathbf{e}_t, \mathbf{R}_t). \quad (21b)$$

The augmented KS requires only $\mathcal{O}(N_x^3 T)$ operations which is much less than the corresponding batch solution in (10).

B. Gauss-Newton IEKS (GN-IEKS) for Non-linear Systems

The solution of (14) has similar computational scaling challenges as the affine case discussed in previous section. However, we can use the equivalence of IEKS and GN [8] to construct an efficient solution for the $\mathbf{x}_{1:T}$ -subproblem. In the IEKS method, we first approximate the non-linear model by linearisation, and then use KS on the linearised model. The $\mathbf{x}_{1:T}$ -subproblem now takes the form of (6a). In an iterated extended Kalman filter, at i :th iteration, we form affine approximations of $\mathbf{a}_t(\mathbf{x}_{t-1})$ and $\mathbf{h}_t(\mathbf{x}_t)$ as follows:

$$\begin{aligned} \mathbf{a}_t(\mathbf{x}_{t-1}) &\approx \mathbf{a}_t(\mathbf{x}_{t-1}^{(i)}) + \mathbf{J}_{a_t}(\mathbf{x}_{t-1}^{(i)}) (\mathbf{x}_{t-1} - \mathbf{x}_{t-1}^{(i)}), \\ \mathbf{h}_t(\mathbf{x}_t) &\approx \mathbf{h}_t(\mathbf{x}_t^{(i)}) + \mathbf{J}_{h_t}(\mathbf{x}_t^{(i)}) (\mathbf{x}_t - \mathbf{x}_t^{(i)}). \end{aligned} \quad (22)$$

We then replace the nonlinear functions in the cost function with the above approximations, and compute the next iterate as the solution to the minimisation problem

$$\begin{aligned} \mathbf{x}_{1:T}^{(i+1)} = & \arg \min_{\mathbf{x}_{1:T}} \frac{1}{2} \left\| \mathbf{y}_t - \mathbf{h}_t(\mathbf{x}_t^{(i)}) + \mathbf{J}_{h_t}(\mathbf{x}_t^{(i)}) (\mathbf{x}_t - \mathbf{x}_t^{(i)}) \right\|_{\mathbf{R}_t^{-1}}^2 \\ & + \frac{1}{2} \sum_{t=2}^T \left\| \mathbf{x}_t - \mathbf{a}_t(\mathbf{x}_{t-1}^{(i)}) + \mathbf{J}_{a_t}(\mathbf{x}_{t-1}^{(i)}) (\mathbf{x}_{t-1} - \mathbf{x}_{t-1}^{(i)}) \right\|_{\mathbf{Q}_t^{-1}}^2 \\ & + \frac{\gamma}{2} \sum_{t=2}^T \|\mathbf{x}_t - \mathbf{B}_t \mathbf{x}_{t-1} - \mathbf{d}_t - \mathbf{v}_t + \bar{\boldsymbol{\eta}}_t / \gamma\|_2^2 \\ & + \frac{\gamma}{2} \|\mathbf{x}_1 - \mathbf{m}_1 - \mathbf{v}_1 + \bar{\boldsymbol{\eta}}_1 / \gamma\|_2^2 + \frac{1}{2} \|\mathbf{x}_1 - \mathbf{m}_1\|_{\mathbf{P}_1^{-1}}^2, \end{aligned} \quad (23)$$

which is equivalent to (18) with

$$\begin{aligned} \mathbf{A}_t &= \mathbf{J}_{a_t}(\mathbf{x}_{t-1}^{(i)}), & \mathbf{b}_t &= \mathbf{a}_t(\mathbf{x}_{t-1}^{(i)}) - \mathbf{J}_{a_t}(\mathbf{x}_{t-1}^{(i)}) \mathbf{x}_{t-1}^{(i)}, \\ \mathbf{H}_t &= \mathbf{J}_{h_t}(\mathbf{x}_t^{(i)}), & \mathbf{e}_t &= \mathbf{h}_t(\mathbf{x}_t^{(i)}) - \mathbf{J}_{h_t}(\mathbf{x}_t^{(i)}) \mathbf{x}_t^{(i)}. \end{aligned} \quad (24)$$

The precise expressions of \mathbf{B}_t and \mathbf{d}_t depend on our choice of sparsity. When \mathbf{q}_t is sparse, the expressions are given by

$$\mathbf{B}_t = \mathbf{J}_{a_t}(\mathbf{x}_{t-1}^{(i)}), \quad \mathbf{d}_t = \mathbf{a}_t(\mathbf{x}_{t-1}^{(i)}) - \mathbf{J}_{a_t}(\mathbf{x}_{t-1}^{(i)}) \mathbf{x}_{t-1}^{(i)}, \quad (25)$$

which needs the same computations as in (19). Thus we can solve the minimisation problem in (6a) by iteratively linearizing the nonlinearities and then by applying KS. This turns out to be mathematically equivalent to applying GN to the batch problem as we did in Section III-C.

C. Levenberg–Marquardt IEKS (LM-IEKS)

There also exists a connection between the Levenberg–Marquardt (LM) and a modified version of IEKS [35]. The LM-IEKS method is based on replacing the minimisation of the approximate cost function in (23) by a regularised minimisation of the form

$$\begin{aligned} \mathbf{x}_{1:T}^* &= \arg \min_{\mathbf{x}_{1:T}} \frac{1}{2} \left\| \mathbf{y}_t - \mathbf{h}_t(\mathbf{x}_t^{(i)}) + \mathbf{J}_{h_t}(\mathbf{x}_t^{(i)}) (\mathbf{x}_t - \mathbf{x}_t^{(i)}) \right\|_{\mathbf{R}_t^{-1}}^2 \\ &+ \frac{1}{2} \sum_{t=2}^T \left\| \mathbf{x}_t - \mathbf{a}_t(\mathbf{x}_{t-1}^{(i)}) + \mathbf{J}_{a_t}(\mathbf{x}_{t-1}^{(i)}) (\mathbf{x}_{t-1} - \mathbf{x}_{t-1}^{(i)}) \right\|_{\mathbf{Q}_t^{-1}}^2 \\ &+ \frac{\gamma}{2} \sum_{t=2}^T \left\| \mathbf{x}_t - \mathbf{B}_t \mathbf{x}_{t-1} - \mathbf{d}_t - \mathbf{v}_t + \frac{\bar{\boldsymbol{\eta}}_t}{\gamma} \right\|_2^2 + \frac{1}{2} \left\| \mathbf{x}_1 - \mathbf{m}_1 \right\|_{\mathbf{P}_1^{-1}}^2 \\ &+ \frac{\lambda^{(i)}}{2} \sum_{t=1}^T \left\| \mathbf{x}_t - \mathbf{x}_t^{(i)} \right\|_{[\mathbf{S}^{(i)}]^{-1}}^2 + \frac{\gamma}{2} \left\| \mathbf{x}_1 - \mathbf{m}_1 - \mathbf{v}_1 + \frac{\bar{\boldsymbol{\eta}}_1}{\gamma} \right\|_2^2, \end{aligned} \quad (26)$$

where we have assume that $\mathbf{S}^{(i)} = \text{diag}(\mathbf{S}_1^{(i)}, \dots, \mathbf{S}_T^{(i)})$. Similarly to GN-IEKS, when \mathbf{B}_t and \mathbf{d}_t are non-zero, we need to build a new state-space model in order to have only one dynamic model. Following [35], the regularisation can be implemented by defining an additional pseudo-measurement $\mathbf{z}_t = \mathbf{x}_t^{(i)}$ with a noise covariance $\boldsymbol{\Sigma}_t^{(i)} = \mathbf{S}_t^{(i)} / \lambda^{(i)}$. Using (24) and (19), we have the augmented state-space model

$$\begin{aligned} p(\mathbf{x}_t | \mathbf{x}_{t-1}) &= \mathcal{N}(\mathbf{x}_t | \tilde{\mathbf{A}}_t \mathbf{x}_{t-1} + \tilde{\mathbf{b}}_t, \tilde{\mathbf{Q}}_t), \\ p(\mathbf{y}_t | \mathbf{x}_t) &= \mathcal{N}(\mathbf{y}_t | \mathbf{H}_t \mathbf{x}_t + \mathbf{e}_t, \mathbf{R}_t), \\ p(\mathbf{z}_t | \mathbf{x}_t) &= \mathcal{N}(\mathbf{z}_t | \mathbf{x}_t, \boldsymbol{\Sigma}_t^{(i)}), \end{aligned} \quad (27)$$

which provides the minimum of the cost function as the KS solution. By combining this with $\lambda^{(i)}$ adaptation and iterating we can implement the LM algorithm for the $\mathbf{x}_{1:T}$ -subproblem using the recursive smoother (cf. [35]).

V. CONVERGENCE ANALYSIS

In this section, we present theoretical convergence results for the proposed methods. Although convergence of multi-block ADMM has already been proven [36], [37], the existing results rely on strong assumptions such as Lipschitz continuity or convexity. Here, we have a milder assumption of amenability [38].

When the functions $\mathbf{a}_t(\mathbf{x}_{t-1})$ and $\mathbf{h}_t(\mathbf{x}_t)$ are affine (see equation (8)), we have the following theorem.

Theorem 1 (Convergence of KS-mADMM). *Let \mathbf{Q}_t and \mathbf{P}_1 be positive definite matrices. Then the sequence $\{\mathbf{x}_{1:T}^{(k)}, \mathbf{w}_{1:T}^{(k)}, \mathbf{v}_{1:T}^{(k)}, \boldsymbol{\eta}_{1:T}^{(k)}\}$ generated by KS-mADMM globally converges to a stationary point $(\mathbf{x}_{1:T}^*, \mathbf{w}_{1:T}^*, \mathbf{v}_{1:T}^*, \boldsymbol{\eta}_{1:T}^*)$.*

Proof. The proof is based on the convexity of the cost function. When the conditions \mathbf{Q}_t and \mathbf{P}_1 are positive definite, the function in (4) is convex. Consider the batch form, due to $[\Phi \ 0][0 \ \mathbf{I}]^\top = \mathbf{0}$, we can write \mathbf{x} and \mathbf{w} into one function $\Xi(\mathbf{x}, \mathbf{w})$. Then, the multi-block ADMM is equivalent to the standard ADMM, which globally converges to a stationary point $(\mathbf{x}^*, \mathbf{w}^*, \mathbf{v}^*, \boldsymbol{\eta}^*)$ [32]. As batch mADMM is equivalent to KS-mADMM, then the sequence $\{\mathbf{x}^{(k)}, \mathbf{w}^{(k)}, \mathbf{v}^{(k)}, \boldsymbol{\eta}^{(k)}\}$ and the sequence $\{\mathbf{x}_{1:T}^{(k)}, \mathbf{w}_{1:T}^{(k)}, \mathbf{v}_{1:T}^{(k)}, \boldsymbol{\eta}_{1:T}^{(k)}\}$ are identical. ■

When the functions $\mathbf{a}_t(\mathbf{x}_{t-1})$ and $\mathbf{h}_t(\mathbf{x}_t)$ are non-linear, we suppose that the function

$$s(\mathbf{x}) \triangleq \frac{1}{2} \|\mathbf{y} - \mathbf{h}(\mathbf{x})\|_{\mathbf{R}^{-1}}^2 + \frac{1}{2} \|\mathbf{m} - \mathbf{a}(\mathbf{x})\|_{\mathbf{Q}^{-1}}^2 \quad (28)$$

is *strongly amenable* [38] at \mathbf{x} . Due to the strongly amenability, the function $s(\mathbf{x})$ will be *prox-regular* [39]. Let $\delta_+(\mathbf{A})$ denote the smallest eigenvalue of \mathbf{A} . We are now ready for introducing the following lemma.

Lemma 1 (Bounded and nonincreasing sequence). *Assume that $\delta_+(\Phi^\top \Phi) > 0$ and $s(\mathbf{x})$ be strongly amenable. Then there exists $\gamma > 0$ such that sequence $\mathcal{L}_\gamma(\mathbf{x}^{(k)}, \mathbf{w}^{(k)}, \mathbf{v}^{(k)}, \boldsymbol{\eta}^{(k)})$ is bounded and nonincreasing.*

Proof. See Appendix A. ■

We next present the main theoretical results.

Theorem 2 (Convergence of GN-IEKS-mADMM). *Let the assumptions in Lemma 1 be satisfied. Then there exists $\gamma > 0$ such that the sequence $\{\mathbf{x}_{1:T}^{(k)}, \mathbf{w}_{1:T}^{(k)}, \mathbf{v}_{1:T}^{(k)}, \boldsymbol{\eta}_{1:T}^{(k)}\}$ generated by GN-IEKS-mADMM locally converges to a local minimum $(\mathbf{x}_{1:T}^*, \mathbf{w}_{1:T}^*, \mathbf{v}_{1:T}^*, \boldsymbol{\eta}_{1:T}^*)$.*

Proof. By Lemma 1, the sequence $\mathcal{L}_\gamma(\mathbf{x}^{(k)}, \mathbf{w}^{(k)}, \mathbf{v}^{(k)}, \boldsymbol{\eta}^{(k)})$ is bounded and nonincreasing. Based on our paper [14], the \mathbf{x} -subproblem has a local minimum \mathbf{x}^* . The \mathbf{w} and \mathbf{v} subproblems are convex [40]. We then conclude that the iterative sequence $\{\mathbf{x}^{(k)}, \mathbf{w}^{(k)}, \mathbf{v}^{(k)}, \boldsymbol{\eta}^{(k)}\}$ locally converges to a local minimum $(\mathbf{x}^*, \mathbf{w}^*, \mathbf{v}^*, \boldsymbol{\eta}^*)$. According to [8], GN is equivalent to IEKS. Thus we deduce that the iterative sequence $\{\mathbf{x}_{1:T}^{(k)}, \mathbf{w}_{1:T}^{(k)}, \mathbf{v}_{1:T}^{(k)}, \boldsymbol{\eta}_{1:T}^{(k)}\}$ is convergent to a local minimum $(\mathbf{x}_{1:T}^*, \mathbf{w}_{1:T}^*, \mathbf{v}_{1:T}^*, \boldsymbol{\eta}_{1:T}^*)$. ■

Lemma 2 (Convergence of LM). *Assume that the norm of Hessian $\mathbf{H}_\theta(\mathbf{x})$ is bounded by a positive constant $\kappa < \max\{\gamma \delta_+(\Phi^\top \Phi), \lambda^{(i)} \delta_+([\mathbf{S}^{(i)}]^{-1})\}$. Then LM is locally (linearly) convergent. The convergence is quadratic when $\kappa \rightarrow 0$.*

Proof. See Appendix B. ■

Theorem 3 (Convergence of LM-IEKS-mADMM). *Let the assumptions of Lemmas 1 and 2 be satisfied. Then there exists $\lambda^{(i)}, \gamma > 0$ such that the sequence $\{\mathbf{x}_{1:T}^{(k)}, \mathbf{w}_{1:T}^{(k)}, \mathbf{v}_{1:T}^{(k)}, \boldsymbol{\eta}_{1:T}^{(k)}\}$ generated by LM-IEKS-mADMM converges to a local minimum $(\mathbf{x}_{1:T}^*, \mathbf{w}_{1:T}^*, \mathbf{v}_{1:T}^*, \boldsymbol{\eta}_{1:T}^*)$.*

Proof. Similar to Theorem 2, we use Lemma 1 to establish the sequence $\mathcal{L}_\gamma(\mathbf{x}^{(k)}, \mathbf{w}^{(k)}, \mathbf{v}^{(k)}; \boldsymbol{\eta}^{(k)})$ is bounded and nonincreasing. Due to the convexity, the \mathbf{w} and \mathbf{v} subproblems have the local minimum. By Lemma 2, the sequence $\mathbf{x}^{(i)}$ generated by LM converges to \mathbf{x}^* . Then the sequence $\{\mathbf{x}^{(k)}, \mathbf{w}^{(k)}, \mathbf{v}^{(k)}, \boldsymbol{\eta}^{(k)}\}$ locally converges to a minimum $(\mathbf{x}^*, \mathbf{w}^*, \mathbf{v}^*, \boldsymbol{\eta}^*)$. Since the sequence $\{\mathbf{x}^{(k)}, \mathbf{w}^{(k)}, \mathbf{v}^{(k)}, \boldsymbol{\eta}^{(k)}\}$ generated by LM is identical to $\{\mathbf{x}_{1:T}^{(k)}, \mathbf{w}_{1:T}^{(k)}, \mathbf{v}_{1:T}^{(k)}, \boldsymbol{\eta}_{1:T}^{(k)}\}$ generated by LM-IEKS [8], [35]. ■

VI. NUMERICAL EXPERIMENTS

In this section, we experimentally evaluate the proposed methods in a selection of different applications, including multi-sensor range measurement problems, ship trajectory-tracking, audio restoration, and autonomous vehicle tracking.

A. Multi-Sensor Range Measurement Problems

In this experiment, we consider a multi-sensor range measurement problem where we have short periods of movement with regular interruptions. This problem frequently appears in many surveillance systems [3], [6]. The state \mathbf{x}_t contains the position $(x_{t,1}, x_{t,2})$ and the velocities $(x_{t,3}, x_{t,4})$. The measurement dynamic model for sensor $n \in \{1, 2, 3\}$ is given by

$$\mathbf{h}_t^n(\mathbf{x}_t) = \sqrt{(x_{t,2} - s_y^n)^2 + (x_{t,1} - s_x^n)^2},$$

where $\Delta t = 0.1$, and (s_x^n, s_y^n) is the position of the sensor n . The transition function $\mathbf{a}_t(\mathbf{x}_{t-1})$ is

$$\mathbf{a}_t(\mathbf{x}_{t-1}) = \begin{bmatrix} 1 & 0 & \Delta t & 0 \\ 0 & 1 & 0 & \Delta t \\ 0 & 0 & 1 & 0 \\ 0 & 0 & 0 & 1 \end{bmatrix} \mathbf{x}_{t-1}, \quad (29)$$

and the covariances are $\mathbf{R}_t = \text{diag}(0.2^2, 0.2^2)$, and $\mathbf{Q}_t = \text{diag}(0.01, 0.01, 0.1, 0.1)$. We assume the target has many interruptions, which means the velocities $x_{t,3}, x_{t,4}$ are sparse. We set $\mathbf{G}_{g,t} = \begin{bmatrix} 0 & 0 & 1 & 0 \\ 0 & 0 & 0 & 1 \end{bmatrix}$, and use the parameters $\gamma = 1$, $\mu = 1$, and $T = 40$. For evaluating the localization performance, we define the *relative error* as $\mathbf{x}_{\text{err}} = \frac{\sum_{t=1}^T \|\mathbf{x}_t^{(k)} - \mathbf{x}_t^{\text{true}}\|_2}{\sum_{t=1}^T \|\mathbf{x}_t^{\text{true}}\|_2}$, where $\mathbf{x}_t^{\text{true}}$ is the ground truth. We then plot the velocity variable $x_{t,3}$ corresponding to the time step t in Fig. 1, which indicates that our method can generate much more sparse results.

Fig. 2 shows the relative error \mathbf{x}_{err} as a function of the iteration number. The values of \mathbf{x}_{err} generated by the regularisation methods are below those generated by iterated extended Kalman smoother (IEKS) [1]. It also shows that the GN-mADMM, GN-IEKS-mADMM, LM-mADMM and LM-IEKS-mADMM can get the optimal values at around 50 iterations. IEKS is the fastest method, but the relative error is highest due to lack of the sparsity prior (i.e., $\mu = 0$). GN-mADMM and GN-IEKS-mADMM have the same convergence rate (as they are equivalent), while the latter uses the less running time. Similarly, LM-IEKS-mADMM needs less time to obtain the result than LM-mADMM. When the number of time steps T is moderate, all the running time are acceptable.

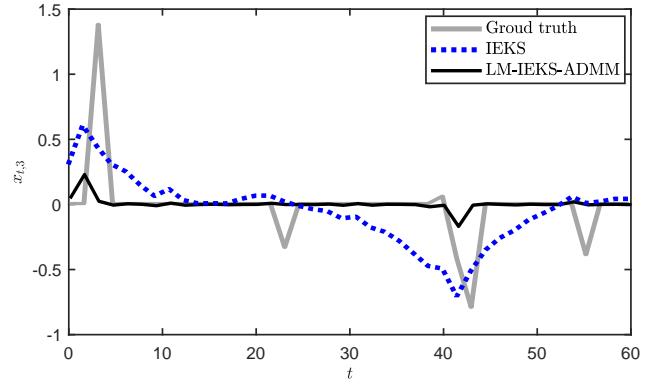


Fig. 1. The estimated trajectory in the non-linear system. The relative errors are 0.53 and 0.46 generated by IEKS and LM-IEKS-ADMM.

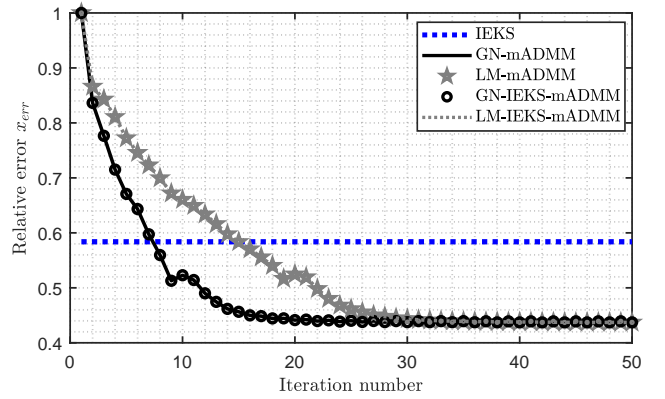


Fig. 2. Relative error \mathbf{x}_{err} versus iteration number.

But when T is extremely large, the proposed methods provide a massive advantage.

Fig. 3 demonstrates how the running time (sec) grows when T is increasing. The proposed methods are compared with the state-of-the-art methods, including the proximal ADMM (prox-ADMM) [31], mADMM [32], and IEKS [1]. Despite being mathematically equivalent, GN-mADMM and GN-IEKS-mADMM, LM-mADMM and LM-IEKS-mADMM, have very different running times. GN-IEKS-mADMM and LM-IEKS-mADMM are more efficient than the batch methods. Due to limited memory, we cannot report the results of the batch methods when $T \geq 10^4$. It is reasonable to conclude that in general, the proposed methods are competitive for extremely large-scale tracking and estimation problems. This approach is computationally inexpensive, which makes it suitable for solving real-world applications, such as ship trajectory-tracking in the next section.

B. Marine Vessel Tracking

In this experiment, we utilise the Wiener velocity model [6] with a sparse noise assumption to track a marine vessel trajectory. The latitude, longitude, speed, and course of the vessel have been captured by automatic identification system (AIS) equipment, collected by Danish Maritime Authority. Similar applications can be found in [5], [30]. The state

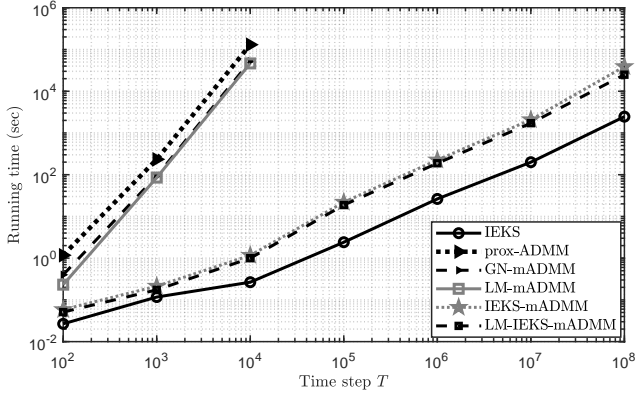


Fig. 3. Comparison of the running times in the range measurement example as function of the number of time steps (from 10^2 to 10^8).

of the ship is measured at time intervals of 1 minute. We assume the process noise \mathbf{q}_t is sparse, and set $\mathbf{G}_{g,t}$ to an identity matrix and use the parameters $\gamma = 1$, $\mu = 1$, and $K_{\max} = 100$. The measurement data consists of 100 time points of the vessel locations. Our method obtains the position estimates as shown in Fig. 4. Fig. 5 shows that our method has sparser process noise than estimated by a Kalman smoother (KS) [1]. We then highlight the computation advantage of our method. The difference in running time is dominated by the $\mathbf{x}_{1:T}$ -subproblem. The running times of KS, prox-ADMM, mADMM, and KS-mADMM, were 0.34s, 174s, 172s, and 5.63s, respectively. The running times of mADMM and prox-ADMM are similar whereas KS-mADMM has a smaller running time that resembles a plain Kalman smoother.

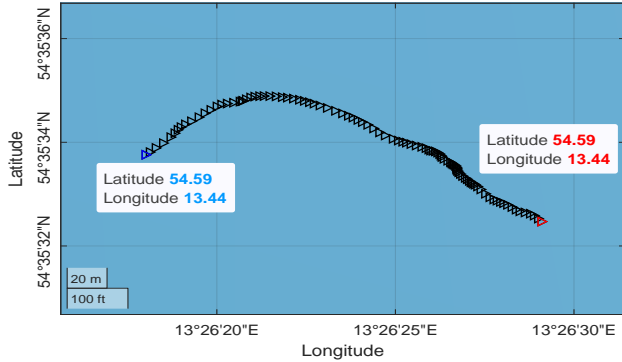


Fig. 4. The position (black markers) estimated by KS-mADMM. The starting coordinate is denoted blue marker, and the ending coordinate is red marker. Contains data from the Danish Maritime Authority that is used in accordance with the conditions for the use of Danish public data.

C. Autonomous Vehicle Tracking

To see how our methods can speed up larger scale real-world problems, we apply GN-IEKS-mADMM to a vehicle tracking problem using real-world data. Global positioning system (GPS) data was collected in urban streets and roads around Helsinki, Finland [41]. The urban environment contained many stops to traffic lights, crossings, turns, and various other non-linear situations. We ran the experiment using a coordinate

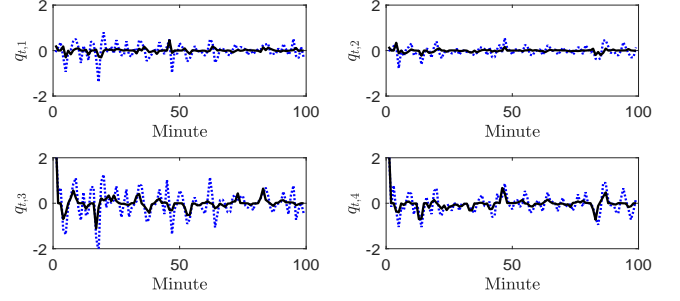


Fig. 5. The process noise estimated by KS-mADMM (black line) and Kalman smoother (blue dash line).

turn model [1], where the state at time step t had the positions $(x_{t,1}, x_{t,2})$, the velocities $(x_{t,3}, x_{t,4})$, and the angle $x_{t,5}$. The number of time points T was 6865. The method parameters are $\gamma = 0.1$, $\mu = 1$, $K_{\max} = 300$ and $I_{\max} = 5$. We utilised

the matrix $\mathbf{G}_{g,t} = \begin{bmatrix} 0 & 0 & 1 & 0 & 0 \\ 0 & 0 & 0 & 1 & 0 \\ 0 & 0 & 0 & 0 & 1 \end{bmatrix}$, to enforce the sparsity

of the velocities and the angle. The plot in Fig. 6 demonstrates the path (blue line) generated by our method. The running time of IEKS [25], GN-mADMM, and GN-IEKS-mADMM were 22s, 13520s and 2704s, respectively. As we expected, although IEKS is fastest, the L_2 -penalised regularisation methods push more of the velocities and the angle to zero, which is shown in Fig. 7. The IEKS estimate has many large peaks that appear as a result of large residuals, and GN-IEKS-mADMM has more sparse results.

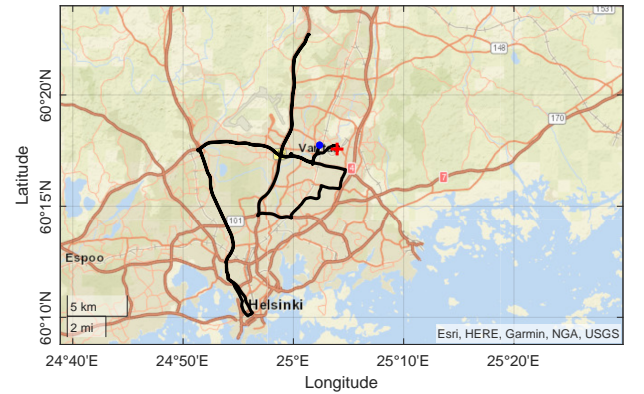


Fig. 6. The path tracking (black line) generated by GN-IEKS-mADMM. The starting position is blue point, and the ending position is red cross.

D. Audio Signal Restoration

The proposed technique can be readily applied to the problem of noise reduction in audio signals using the Gabor regression model [42]:

$$y(\tau) = \sum_{m=0}^{M/2} \sum_{n=0}^{N-1} c_{m,n} g_{m,n}(\tau) + r(\tau), \quad \tau = 0, \dots, T-1$$

where signals are represented as a weighted sum of Gabor atoms $g_{m,n}(\tau) = w_n(\tau) \exp(2\pi i \frac{m}{M} \tau)$. Terms $w_n(\tau)$ correspond to a window function with bounded support centered at

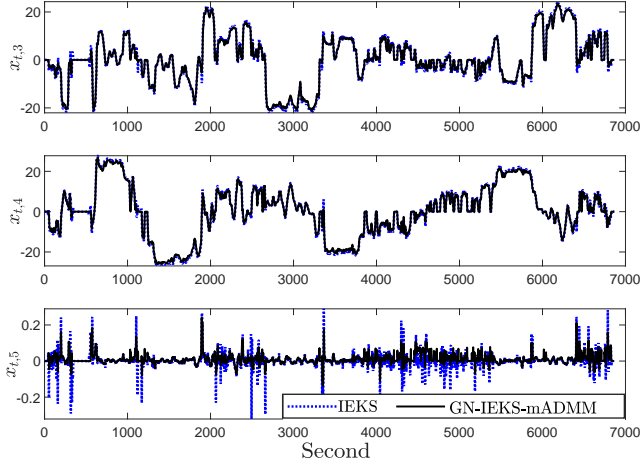


Fig. 7. The estimated velocities and angular velocities generated by IEKS (blue dash line) and the proposed method (black line).

time instants τ_n , whose values are chosen such that the time axis is tiled with evenly spaced overlapping frames. Sparsity is promoted through the L_2^1 pair-wise grouping pattern described in Section II: $\sum_{m,n} \mu_{m,n} \|c_{m,n}\|_2$, where the real representation of complex coefficients $c_{m,n}$ used in [42] is adopted. This batch problem is restated in terms of a state-space model. Signal \mathbf{y} is separated into P chunks \mathbf{y}_t of length L (window size) and state vectors $\mathbf{x}_t = [\mathbf{c}_{2(t-1)}; \mathbf{c}_{2t-1}; \mathbf{c}_{2t}]^T$ are defined, \mathbf{c}_t being the subvector associated to each frame. Let \mathbf{H}_0 be a matrix having the non-zero values of the Gabor atoms of the first frame $\mathbf{g}_{0,0}, \dots, \mathbf{g}_{M/2,0}$ as columns. Thus, atoms in subsequent frames are time-shifted replicas of this basic set and $\|\mathbf{y} - \mathbf{D}\mathbf{c}\|^2$ (\mathbf{D} a matrix arrangement of the original Gabor atoms, a dictionary matrix) can be replaced by $\sum_{t=1}^P \|\mathbf{y}_t - \mathbf{H}_* \mathbf{x}_t\|^2 + \sum_{t=1}^P \|\mathbf{x}_t - \mathbf{A}_t \mathbf{x}_{t-1}\|^2$, with $\mathbf{H}_* = [\mathbf{H}_u, \mathbf{H}_0, \mathbf{H}_\ell]$ and $\mathbf{A}_t = [\mathbf{0}, \mathbf{0}, \mathbf{0}; \mathbf{0}, \mathbf{0}, \mathbf{0}; \mathbf{I}, \mathbf{0}, \mathbf{0}]$. Terms $\mathbf{H}_u, \mathbf{H}_\ell$ are truncated versions of \mathbf{H}_0 corresponding to the contribution of the adjacent overlapping frames.

The algorithm is tested on a ~ 2.65 second long glockenspiel excerpt sampled at 22050 [Hz] and contaminated with artificial background noise with signal-to-noise ratio (SNR) 5dB. Experiments are carried out in an Intel Core i7 @ 2.50GHz, 16 GB RAM, with parameters $\gamma = 5$, $\mu = 3.7$, and $K_{\max} = 500$ (longer runs do not improve the results noticeably) and a window length of 512 samples. Kalman gain matrices are pre-computed. Output SNR is 11.04 with an average running time of 74s (20 repetitions). Fig. 8 shows the visual reconstruction results. In comparison, Gibbs sampling schemes to compute similar models (e.g., [42]) yield noisier restorations for the same computing time¹. Reflecting the power spectrum of typical audio signals, which decays with frequency, penalisation is made frequency-dependent by setting $\mu_{m,n} = \mu/f(m)$, with $f(m)$ a decreasing modulating function (e.g., a Butterworth filter gain). Devising appropriate temporal evolution models for the audio synthesis coefficients over time (e.g., as done in the context of ECG signal analysis [18]) and investigating a self-adaptive scheme for the estimation of μ (here tuned

empirically) are topics of future research.

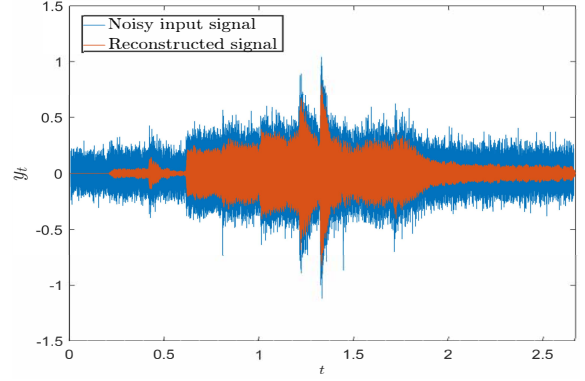


Fig. 8. Reconstructed glockenspiel excerpt.

VII. CONCLUSION

In this paper, we have presented efficient smoothing-and-splitting methods for solving regularised autonomous tracking and state estimation problems. We formulated the general problem as a generalised L_2 -penalised dynamic group Lasso type of minimisation problem. The problem can be solved using batch methods when the number of time steps is moderate. For the case with a large number of time steps, new KS-mADMM, GN-IEKS-mADMM, and LM-IEKS-mADMM methods were developed. We also proved the convergence of the methods. We applied the developed methods to simulated and real-world tracking and audio signal restoration problems where methods resulted in improved localization and estimation performance, and a significantly reduced computation load.

APPENDIX A PROOF OF LEMMA 1

To simplify the notation, we replace the $(k+1)$: iteration by the $+$:th iteration, and drop the iteration counter k in this proof. Due to the strongly amenability, $s(\mathbf{x})$ is prox-regular with a positive constant M . Now we compute

$$\begin{aligned} & \mathcal{L}(\mathbf{x}, \mathbf{w}, \mathbf{v}; \boldsymbol{\eta}) - \mathcal{L}(\mathbf{x}^{(+)}, \mathbf{w}^{(+)}, \mathbf{v}; \boldsymbol{\eta}) \\ &= s(\mathbf{x}) - s(\mathbf{x}^{(+)}) + \langle \bar{\boldsymbol{\eta}}, \Phi \mathbf{x}^{(+)} - \Phi \mathbf{x} \rangle \\ &+ \langle \gamma(\Phi \mathbf{x}^{(+)} - \mathbf{d} - \mathbf{v}), \Phi \mathbf{x}^{(+)} - \Phi \mathbf{x} \rangle + \frac{\gamma}{2} \|\Omega \mathbf{x}^{(+)} - \Omega \mathbf{x}\|^2 \\ &+ g(\mathbf{w}) - g(\mathbf{w}^{(+)}) + \langle \underline{\boldsymbol{\eta}}, \mathbf{w}^{(+)} - \mathbf{w} \rangle \\ &+ \langle \gamma(\mathbf{w}^{(+)} - \mathbf{G} \mathbf{v}), \mathbf{w}^{(+)} - \mathbf{w} \rangle + \frac{\gamma}{2} \|\mathbf{w}^{(+)} - \mathbf{w}\|^2 \\ &> \frac{\gamma \delta_+ (\Phi^T \Phi) - M}{2} \|\mathbf{x}^{(+)} - \mathbf{x}\|^2 + \frac{\gamma}{2} \|\mathbf{w}^{(+)} - \mathbf{w}\|^2, \end{aligned} \quad (30)$$

where $\boldsymbol{\eta} = \text{vec}(\bar{\boldsymbol{\eta}}, \underline{\boldsymbol{\eta}})$. We then have

$$\begin{aligned} & \mathcal{L}(\mathbf{x}^{(+)}, \mathbf{w}^{(+)}, \mathbf{v}^{(+)}; \boldsymbol{\eta}^{(+)}) - \mathcal{L}(\mathbf{x}, \mathbf{w}, \mathbf{v}; \boldsymbol{\eta}) \\ &< \frac{M - \gamma \delta_+ (\Phi^T \Phi)}{2} \|\mathbf{x}^{(+)} - \mathbf{x}\|^2 \\ &+ \frac{1}{\gamma} \|\boldsymbol{\eta}^{(+)} - \boldsymbol{\eta}\|^2 + \frac{\gamma}{2} \|\mathbf{w}^{(+)} - \mathbf{w}\|^2, \end{aligned} \quad (31)$$

¹Input and code in https://github.com/matclaveria/admm_denoising

which will be nonnegative provided when $\gamma > \frac{M}{\delta_+(\Phi^\top \Phi)} > 0$ is satisfied. In particular, when $\Phi = \mathbf{I}$, $\delta_+(\Phi^\top \Phi) = 1$.

In our case, $\mathcal{L}(\mathbf{x}^{(k)}, \mathbf{w}^{(k)}, \mathbf{v}^{(k)}; \boldsymbol{\eta}^{(k)})$ is upper bounded by $\mathcal{L}(\mathbf{x}^{(0)}, \mathbf{w}^{(0)}, \mathbf{v}^{(0)}; \boldsymbol{\eta}^{(0)})$, and is also lower bounded by $\mathcal{L}(\mathbf{x}^{(k)}, \mathbf{w}^{(k)}, \mathbf{v}^{(k)}; \boldsymbol{\eta}^{(k)}) \geq s(\mathbf{x}^{(k)}) + \sum_{t=1}^T \sum_{g=1}^{N_g} \mu \|\mathbf{w}_{g,t}\|_2$. Thus, we get the conclusion.

APPENDIX B PROOF OF LEMMA 2

We use the smallest non-zero eigenvalue of $\Phi^\top \Phi$ and \mathbf{S}^{-1} to yield the inequality

$$\left\| \mathbf{J}_\theta^\top \mathbf{J}_\theta(\mathbf{x}^{(i)}) \right\| \geq \max \left\{ \gamma \delta_+(\Phi^\top \Phi), \lambda^{(i)} \delta_+([\mathbf{S}^{(i)}]^{-1}) \right\}, \quad (32)$$

where $\mathbf{J}_\theta = [\mathbf{R}^{-\frac{1}{2}} \mathbf{J}_h(\mathbf{x}) \quad \mathbf{Q}^{-\frac{1}{2}} \mathbf{J}_a(\mathbf{x}) \quad \gamma^{\frac{1}{2}} \Phi \quad \lambda^{\frac{1}{2}} \mathbf{S}^{-\frac{1}{2}}]^\top$. We then have

$$\begin{aligned} \left\| \mathbf{x}^{(i+1)} - \mathbf{x}^* \right\| &\leq \frac{M}{2} \left\| [\mathbf{J}_\theta^\top \mathbf{J}_\theta(\mathbf{x}^{(i)})]^{-1} \right\| \left\| \mathbf{x}^{(i)} - \mathbf{x}^* \right\|^2 \\ &\quad + \left\| [\mathbf{J}_\theta^\top \mathbf{J}_\theta(\mathbf{x}^{(i)})]^{-1} \mathbf{H}_\theta(\mathbf{x}^{(i)}) \right\| \left\| \mathbf{x}^{(i)} - \mathbf{x}^* \right\|. \end{aligned} \quad (33)$$

When $\|\mathbf{H}_\theta(\mathbf{x})\| \leq \kappa$ and $\kappa \rightarrow 0$, the convergence is quadratic. The linear convergence can be established when the inequality $\left\| [\mathbf{J}_\theta^\top \mathbf{J}_\theta(\mathbf{x}^{(i)})]^{-1} \mathbf{H}_\theta(\mathbf{x}^{(i)}) \right\| \leq \kappa / \max \left\{ \gamma \delta_+(\Phi^\top \Phi), \lambda^{(i)} \delta_+([\mathbf{S}^{(i)}]^{-1}) \right\} < 1$, is satisfied.

REFERENCES

- [1] S. Särkkä, *Bayesian Filtering and Smoothing*. Cambridge Univ. Press, Aug. 2013.
- [2] F. Dornaika and B. Raducanu, "Three-dimensional face pose detection and tracking using monocular videos: Tool and application," *IEEE Trans. Syst., Man, Cybern. B, Cybern.*, vol. 39, no. 4, pp. 935–944, Aug. 2009.
- [3] G. Rogez, J. Rihan, J. J. Guerrero, and C. Orrite, "Monocular 3-D gait tracking in surveillance scenes," *IEEE Trans. Cybern.*, vol. 44, no. 6, pp. 894–909, Jun. 2014.
- [4] S. J. Godsill and P. J. Rayner, *Digital Audio Restoration: A Statistical Model Based Approach*. New York: Springer-Verlag, 1998.
- [5] B. I. Ahmad, J. K. Murphy, P. Langdon, S. Godsill, R. Hardy, and L. Skrypchuk, "Intent inference for hand pointing gesture-based interactions in vehicles," *IEEE Trans. Cybern.*, vol. 46, no. 4, pp. 878–889, Apr. 2016.
- [6] Y. B. Shalom, X. Li, and T. Kirubarajan, *Estimation with Applications to Tracking and Navigation*. Wiley, 2001.
- [7] H. E. Rauch, F. Tung, and C. T. Striebel, "Maximum likelihood estimates of linear dynamic system," *AIAA J.*, vol. 3, no. 8, pp. 1445–1450, Aug. 1965.
- [8] B. Bell, "The iterated Kalman smoother as a Gauss-Newton method," *SIAM J. Optim.*, vol. 4, no. 3, pp. 626–636, Aug. 1994.
- [9] T. D. Barfoot, "State estimation for robotics," *Cambridge Univ. Press*, 2017.
- [10] Á. F. García-Fernández, L. Svensson, and S. Särkkä, "Cooperative localisation using posterior linearisation belief propagation," *IEEE Trans. Veh. Technol.*, vol. 67, no. 1, pp. 832–836, Jan. 2018.
- [11] W. Li, G. Wei, F. Han, and Y. Liu, "Weighted average consensus-based unscented Kalman filtering," *IEEE Trans. Cybern.*, vol. 46, no. 2, pp. 558–567, Feb. 2016.
- [12] S. Seifzadeh, B. Khaleghi, and F. Karray, "Distributed soft-data-constrained multi-model particle filter," *IEEE Trans. Cybern.*, vol. 45, no. 3, pp. 384–394, Mar. 2015.
- [13] J. Chen, J. H. Li, S. H. Yang, and F. Deng, "Weighted optimization-based distributed Kalman filter for nonlinear target tracking in collaborative sensor networks," *IEEE Trans. Cybern.*, vol. 47, no. 11, pp. 3892–3905, Nov. 2017.
- [14] R. Gao, F. Tronarp, and S. Särkkä, "Iterated extended Kalman smoother-based variable splitting for L1-regularized state estimation," *IEEE Trans. Signal Process.*, vol. 97, no. 19, pp. 5078–5092, Oct. 2019.
- [15] J. Tisdale, Z. Kim, and J. Hedrick, "Autonomous UAV path planning and estimation," *IEEE Robot. Autom. Mag.*, vol. 16, no. 2, pp. 35–42, Jun. 2009.
- [16] P. J. Wolfe and S. J. Godsill, "Interpolation of missing data values for audio signal restoration using a gabor regression model," in *Proc. IEEE Int. Conf. Acoust., Speech, Signal Process.* IEEE, 2005, pp. 517–520.
- [17] J. Murphy and S. Godsill, "Joint bayesian removal of impulse and background noise," in *Proc. IEEE Int. Conf. Acoust., Speech, Signal Process.* IEEE, 2011, pp. 261–264.
- [18] Z. Zhao, S. Särkkä, and A. B. Rad, "Spectro-temporal ECG analysis for atrial fibrillation detection," in *IEEE 28th Int. Workshop on Machine Learning for Signal Process.*, 2018, pp. 1–6.
- [19] R. Gao, F. Tronarp, Z. Zhao, and S. Särkkä, "Regularized state estimation and parameter learning via augmented Lagrangian Kalman smoother method," in *IEEE 29th Int. Workshop on Machine Learning for Signal Process.*, Pittsburgh, PA, USA, Oct. 2019.
- [20] R. Tibshirani, "Regression shrinkage and selection via the lasso," *Journal of the Royal Statistical Society*, vol. 58, no. 1, pp. 267–288, 1996.
- [21] L. Meier, S. van de Geer, and P. Bühlmann, "The group LASSO for logistic regression," *J. Roy. Stat. Soc. B*, vol. 70, no. 1, pp. 53–71, 2008.
- [22] L. I. Rudin, S. Osher, and E. Fatemi, "Nonlinear total variation-based noise removal algorithms," *Physica D*, vol. 60, no. 1–4, pp. 259–268, 1992.
- [23] S. Farahmand, G. Giannakis, and D. Angelosante, "Doubly robust smoothing of dynamical processes via outlier sparsity constraints," *IEEE Trans. Signal Process.*, vol. 59, no. 10, pp. 4529–4543, Oct. 2011.
- [24] A. Simonetto and E. Dall'Anese, "Prediction-correction algorithms for time-varying constrained optimization," *IEEE Trans. Signal Process.*, vol. 65, no. 20, pp. 942–952, Oct. 2017.
- [25] A. Aravkin, J. V. Burke, L. Ljung, A. Lozano, and G. Pillonetto, "Generalized Kalman smoothing: modeling and algorithms," *Automatica*, vol. 86, pp. 63–86, Dec. 2017.
- [26] A. S. Charles, A. Balavoine, and C. J. Rozell, "Dynamic filtering of time-varying sparse signals via L1 minimization," *IEEE Trans. Signal Process.*, vol. 64, no. 21, pp. 5644–5656, Nov. 2016.
- [27] L. Wu, Y. Wang, and S. Pan, "Exploiting attribute correlations: A novel trace lasso-based weakly supervised dictionary learning method," *IEEE Trans. Cybern.*, vol. 47, no. 12, pp. 4497–4508, Dec. 2017.
- [28] T. Bai, Y.-F. Li, and X. Zhou, "Learning local appearances with sparse representation for robust and fast visual tracking," *IEEE Trans. Cybern.*, vol. 45, no. 4, pp. 663–675, Apr. 2015.
- [29] B. S. Park and S. J. Yoo, "An error transformation approach for connectivity-preserving and collision-avoiding formation tracking of networked uncertain underactuated surface vessels," *IEEE Trans. Cybern.*, vol. 49, no. 8, pp. 2955–2966, Aug. 2019.
- [30] J. C. McCall and M. M. Trivedi, "Integral line-of-sight guidance and control of underactuated marine vehicles: Theory simulations and experiments," *IEEE Trans. Control Syst. Technol.*, vol. 24, no. 5, pp. 1623–1642, Sep. 2016.
- [31] S. J. Wright and J. Nocedal, *Numerical Optimization*. Springer Verlag, 2006.
- [32] S. Boyd, N. Parikh, E. Chu, B. Peleato, and J. Eckstein, "Distributed optimization and statistical learning via the alternating direction method of multipliers," *Foundations and Trends in Machine Learning*, vol. 3, no. 1, pp. 1–122, 2011.
- [33] A. T. Puig, A. Wiesel, G. Fleury, and A. O. Hero, "Multidimensional shrinkage-thresholding operator and group LASSO penalties," *IEEE Signal Process. Lett.*, vol. 18, no. 6, pp. 363–366, 2011.
- [34] J. J. Moré, "The Levenberg-Marquardt algorithm: Implementation and theory," *Numerical Analysis*, pp. 105–116, 1978.
- [35] S. Särkkä and L. Svensson, "Levenberg-Marquardt and line-search extended Kalman smoothers," in *Proc. IEEE Int. Conf. Acoust., Speech, Signal Process.* Barcelona, Spain: IEEE, 2020.
- [36] C. Chen, B. He, Y. Ye, and X. Yuan, "The direct extension of ADMM for multi-block convex minimization problems is not necessarily convergent," *Math. Program.*, vol. 155, pp. 57–79, 2016.
- [37] B. He and X. Yuan, "A class of ADMM-based algorithms for three-block separable convex programming," *Comput. Optim. Appl.*, vol. 70, no. 3, pp. 791–826, Jul. 2018.
- [38] R. T. Rockafellar and R. Wets, "Variational analysis," *Berlin, Germany: Springer Verlag*, 1998.
- [39] R. A. Poliquin and R. T. Rockafellar, "Prox-regular functions in variational analysis," *Trans. AMS*, vol. 348, pp. 1805–1838, 1996.
- [40] S. Boyd and L. Vandenberghe, *Convex Optimization*. Cambridge Univ. Press, 2004.

- [41] J. Hartikainen and S. Särkkä, “Sequential inference for latent force models,” *Proc. 27th Conf. Uncertainty in Artificial Intelligence*, pp. 311–318, 2011.
- [42] P. J. Wolfe, S. J. Godsill, and W.-J. Ng, “Bayesian variable selection and regularization for time–frequency surface estimation,” *Journal of the Royal Statistical Society: Series B*, vol. 66, no. 3, pp. 575–589, 2004.